Proc. Natl. Acad. Sci. USA
Vol. 88, pp. 2903–2907, April 1991
Biochemistry

Structural similarities in glutaminyl- and methionyl-tRNA synthetases suggest a common overall orientation of tRNA binding

(protein–nucleic acid recognition/protein structure alignment/aminoacyl-tRNA synthetases)

JOHN J. PERONA[†‡], MARK A. ROULD[†], THOMAS A. STEITZ[†§], JEAN-LOUP RISLER[¶], CHARLES ZELWER[¶], AND SIMONE BRUNIE[‖]

[†]Department of Molecular Biophysics and Biochemistry, and Howard Hughes Medical Institute, Yale University, New Haven, CT 06511; [¶]Centre de Génétique Moléculaire, Centre National de la Recherche Scientifique, Laboratoire Associé a l'Université de Paris VI, 91198 Gif-sur-Yvette Cedex, France; and [‖]Laboratoire de Biochimie (Centre National de la Recherche Scientifique Unite de Recherche Associeé 240), Ecole Polytechnique, 91128 Palaiseau Cedex, France

Contributed by Thomas A. Steitz, December 26, 1990

ABSTRACT **Detailed comparisons between the structures of the tRNA-bound *Escherichia coli* glutaminyl-tRNA (Gln-tRNA) synthetase [L-glutamine:tRNA^{Gln} ligase (AMP-forming), EC 6.1.1.18] and recently refined *E. coli* methionyl-tRNA (Met-tRNA) synthetase [L-methionine:tRNA^{Met} ligase (AMP-forming), EC 6.1.1.10] reveal significant similarities beyond the anticipated correspondence of their respective dinucleotide-fold domains. One similarity comprises a 23-amino acid α-helix–turn–β-strand motif found in each enzyme within a domain that is inserted between the two halves of the dinucleotide binding fold. A second correspondence, which consists of two α-helices connected by a large loop and β-strand, is located in the Gln-tRNA synthetase within a region that binds the inside corner of the "L"-shaped tRNA molecule. This structural motif contains a long α-helix, which extends along the entire length of the D and anticodon stems of the complexed tRNA. We suggest that the positioning of this helix relative to the dinucleotide fold plays a critical role in ensuring the proper global orientation of tRNA^{Gln} on the surface of the enzyme. The structural correspondences suggest a similar overall orientation of binding of tRNA^{Met} and tRNA^{Gln} to their respective synthetases.**

Aminoacyl-tRNA synthetases comprise a family of related enzymes that function to specifically couple amino acids to their respective transfer RNAs. Despite their common biological role, however, these enzymes exhibit a remarkable variability in size and oligomeric structure (for a review, see ref. 1). Alignment of primary sequences indicates that enzymes from different organisms that catalyze the acylation of the same amino acid usually retain about 30–50% identity at the amino acid level. However, sequence comparisons among enzymes specific for different amino acid substrates have revealed only limited sections of similarity. Nine of the enzymes, those specific for the amino acids glutamine (2), glutamate (3), tyrosine (4), tryptophan (5), methionine (6), isoleucine (7), valine (8), leucine (9), and arginine (10), possess two segments of primary sequence similarity. One segment contains a His-Ile-Gly-His motif found within a conserved stretch of 10–12 amino acids (7); the other may be represented by the consensus sequence Lys-Met-Ser-Lys-Ser (11). Further similarities, consisting of short blocks of sequences dispersed throughout the length of the polypeptides, exist among the *Escherichia coli* methionine, isoleucine, valine, and leucine enzymes (12).

The structures of the *E. coli* glutaminyl-tRNA (Gln-tRNA) synthetase [L-glutamine:tRNA^{Gln} ligase (AMP-forming), EC 6.1.1.18] complexed with tRNA^{Gln} and ATP (13) and of a fully active tryptic fragment of the *E. coli* methionyl-tRNA (Met-tRNA) synthetase [L-methionine:tRNA^{Met} ligase (AMP-forming), EC 6.1.1.10] in the presence of ATP (14) have been described recently. For each enzyme, comparisons with the refined structure of the *Bacillus stearothermophilus* tyrosyl-tRNA (Tyr-tRNA) synthetase (EC 6.1.1.1) (15) have revealed the common presence of a structurally homologous dinucleotide, or Rossmann, fold in which the catalytic sites reside. In all three enzymes, the fold is located at the amino terminus and possesses an insertion between its two symmetrically related halves. In Gln-tRNA synthetase, this inserted domain plays a critical role in binding a distorted conformation of the 3′ acceptor strand of the tRNA (13). The mode of binding of the adenosine monophosphate moieties of ATP to Gln-tRNA synthetase and tyrosyl adenylate to Tyr-tRNA synthetase were seen to be similar (13). However, a comparison of the Tyr-tRNA and Met-tRNA synthetases indicated that, despite the overall structural similarity of the α-carbon backbones in the active-site region, ATP nevertheless was bound in a quite different orientation to the Met-tRNA synthetase (14). The carboxyl-terminal domains of all three enzymes are structurally disparate.

Although there are no detailed structural data available for the interactions of Tyr-tRNA and Met-tRNA with their respective synthetases, a number of genetic and biochemical approaches have produced evidence regarding specific regions of the proteins and RNAs important to recognition (16, 17). In the case of the Met-tRNA synthetase–tRNA^{Met} interaction, chemical cross-linking studies have identified enzyme residues Lys-61 and Lys-335 as being adjacent to the 3′ end of the bound tRNA (17), and site-directed mutagenesis has demonstrated that Lys-335 plays a crucial role in amino acid activation (18). Cross-linking and site-directed mutagenesis studies have also been used to identify residues Trp-461 and Lys-465 as being located near the anticodon of the tRNA (19–21). These data thus establish two widely separated regions of each macromolecule that lie in close proximity to the structural interface that forms upon binding. The role of the anticodon bases in specifying tRNA^{Met} identity has been well established (e.g., ref. 22).

Presented here are the results of a detailed structural comparison between Met-tRNA synthetase and the tRNA-bound conformation of Gln-tRNA synthetase. We find significant structural similarities outside the respective dinucleotide-fold domains of the two enzymes. Together with the aforementioned solution data, this comparative analysis suggests the possibility

The publication costs of this article were defrayed in part by page charge payment. This article must therefore be hereby marked "*advertisement*" in accordance with 18 U.S.C. §1734 solely to indicate this fact.

[‡]Present address: Department of Pharmaceutical Chemistry, University of California, San Francisco, CA 94143-0446.
[§]To whom reprint requests should be addressed.

that a similar overall topology of tRNA interaction exists in both the methionine and glutamine systems.

RESULTS AND DISCUSSION

The structural similarities between the dinucleotide-fold domains of Gln-tRNA synthetase and Met-tRNA synthetase are summarized in Table 1. It is clear that the similarity extends over the entire domain. The structural correspondence is limited to the secondary structure elements, with large variability in the sizes and conformations of the loops bridging these elements. The folds of each enzyme are divided into two halves that are related by a pseudo-dyad axis of symmetry. In the case of the Gln-tRNA synthetase, the two halves are interrupted by the insertion of the 110-amino acid acceptor-binding domain [residues 100–210 (13)], which serves to bind the hairpin conformation adopted by the acceptor strand of the complexed $tRNA^{Gln}$ molecule. The Met-tRNA synthetase fold is interrupted by two insertions, one of which is similarly located between the two symmetrically related halves and the other of which is inserted within the second half (residues 100–193 and 233–303, respectively) (ref. 14; Fig. 1). These two insertions pack against each other to form a single large domain. Interestingly, despite the high degree of structural correspondence within the α-helices and β-strands of the fold, no significant primary sequence similarity in equivalent residues exists beyond the His-Ile-Gly-His motif.

Table 1. Superposition of α-carbon atoms in Gln-tRNA synthetase (reference structure) and Met-tRNA synthetase (trial structure)

Trial structure		Reference structure			
Residues	2° structure†	Residues	2° structure†	No. of residues	rms D, Å
7–11	β-A*	27–31	β-1	5	2.26
13–38	loop, α-HA*	32–57	loop, α-B	26	1.29
45–54	β-B*	59–68	β-2	10	2.43
72–78	α-HB*	77–83	α-C	7	2.30
94–97	β-C*	95–98	β-3	4	3.00
102–124	α-H1, β-S1	102–124	α-D, β-4	23	1.66
227–231	β-D*	226–230	β-9	5	1.40
303–314	α-HD*	238–249	α-H	12	1.54
319–326	β-E*	254–261	β-10	8	2.39
340–349	α-HE*	302–311	α-K	10	1.56
Overall equivalence					
Nucleotide fold only				77	1.73
All superimposed α carbons				110	1.89

The α-carbon backbone atoms were superimposed by using the computer program OVRLAP, which implements the algorithm of Rossmann and Argos (23). Manual superposition of the structures by utilizing the computer program FRODO identified the structural equivalence of six residues in the region of the His-Ile-Gly-His motif (Gln-tRNA synthetase residues 40–45; Met-tRNA synthetase residues 21–26), which were then utilized as a starting point for determination of the full set of equivalencies using OVRLAP. Input coordinate files consisted of all α-carbon atoms of both Gln-tRNA synthetase and Met-tRNA synthetase. Secondary structure designations follow those of Rould *et al.* (13) and Brunie *et al.* (14). Additional structural correspondences exist between α-helices G of Gln-tRNA synthetase (residues 212–222) and C* of Met-tRNA synthetase (residues 195–205); however, these structural elements of the dinucleotide fold were removed from the superposition calculation because of the much larger discrepancy in their relative positions. Underlined correspondences represent structural equivalencies found to be outside of the dinucleotide binding fold domain. rms D, root mean square deviation in the position of the superimposed α-carbon atoms.

†2° structure refers to secondary structure elements. Asterisks refer to the elements of the trial structure (Met-tRNA synthetase). β, β-strand; α, α-helix; nomenclature of strands and helices is according to refs. 13 and 14.

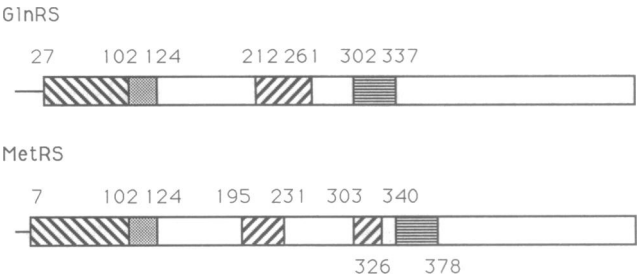

FIG. 1. Structural homologies between Gln-tRNA synthetase and Met-tRNA synthetase. Regions of tertiary structure homology between the two enzymes are indicated by filled boxes: ▧, First half of the dinucleotide fold; ▨, second half of the dinucleotide fold; ▩, α-helix–turn–β-strand motif within the inserted domain between the two halves of the dinucleotide folds; ▤, α-helix–turn–β-strand–α-helix motif found at the inside corner of the L-shaped tRNA molecule in the Gln-tRNA synthetase–$tRNA^{Gln}$ complex.

The superposition of α carbons in the dinucleotide-fold domains of the enzymes revealed in addition an unexpected segment of structural correspondence between amino acids 102 and 124 of both Gln-tRNA synthetase and Met-tRNA synthetase (Figs. 2 and 3). This stretch of 23 residues adopts a common α-helix–turn–β-strand motif in the two enzymes. The structural similarity is extremely good; a superposition of α-carbon atoms of these residues alone gave a rms deviation of 0.6 Å for residues 102–118, with a small divergence in the orientation of the final 6 residues of the β-strand. In each enzyme, these residues follow directly the last β-strand of the first half of the dinucleotide fold and form a solvent-exposed structure that wraps around the back side of the inserted domains (Fig. 1). In Gln-tRNA synthetase, the inserted domain has been termed the acceptor-binding domain (13) because of its function in providing a structure that is complementary to the hairpin conformation of the acceptor strand of the tRNA. However, none of the amino acids in this conserved motif interact directly with the tRNA. Therefore, it seems likely that the motif plays a structural role in stabilizing the overall fold of this domain, which in Gln-tRNA synthetase consists in total of a five-stranded antiparallel β-sheet structure flanked by three α-helices. The conservation of structure between Gln-tRNA synthetase and Met-tRNA synthetase in this region may indicate a common need of the two enzymes to stabilize their inserted domains for interaction with the respective tRNA substrates. Comparison of the primary sequences of the two enzymes in this region reveals no overall similarity; however, a glycine residue is found to be located in each motif at the tight turn connecting the α-helix and β-strand.

Examination of all α-carbon atoms of both enzymes after superimposing the dinucleotide folds resulted in the identification of another region of structural similarity (Table 1 and Figs. 1, 2, and 3). This region consists of an α-helix–turn–β-strand–α-helix motif, which in the Gln-tRNA synthetase–$tRNA^{Gln}$ cocrystal structure is seen to interact with the tRNA at the extreme inside corner of its L-shaped structure. The β-strand element of the motif (residues 317–322 of Gln-tRNA synthetase and 354–359 of Met-tRNA synthetase) is located adjacent to the dinucleotide fold and potentially could be considered as a sixth parallel strand of this domain. In the case of both enzymes, however, the crossover connection from the neighboring strand (β-10 of Gln-tRNA synthetase, β-E* of Met-tRNA synthetase; see Table 1 for meaning of structural notations) is left-handed (14).

In Gln-tRNA synthetase this motif possesses a structure that is complementary to the $tRNA^{Gln}$ substrate in the region

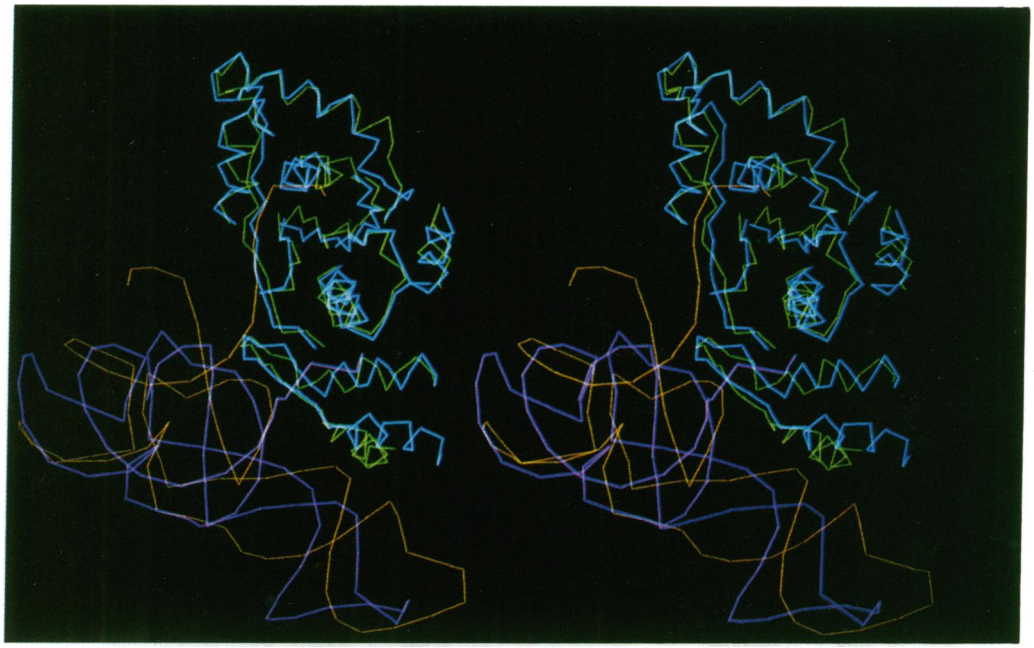

FIG. 2. Superposition of structurally similar regions of Gln-tRNA synthetase and Met-tRNA synthetase. Stereoview of the conserved structural elements in Gln-tRNA synthetase and Met-tRNA synthetase shown in Fig. 1. (Nonconserved loops between secondary structural elements have been omitted for clarity.) The view is oriented along the pseudo-dyad axis of the dinucleotide binding folds of Gln-tRNA synthetase (blue α-carbon trace) and Met-tRNA synthetase (green α-carbon trace). The α-helix–turn–β-strand (residues 102–124 of both Met-tRNA synthetase and Gln-tRNA synthetase, top portion) and α-helix–turn–β-strand–α-helix (residues 340–378 of Met-tRNA synthetase and 302–337 of Gln-tRNA synthetase, bottom portion) motifs, which superimpose together with the dinucleotide folds, are also shown. The phosphate backbone of $tRNA^{Gln}$ as seen in the cocrystal structure with Gln-tRNA synthetase is in orange; the backbone of $tRNA^{Gln}$ docked onto the surface of Met-tRNA synthetase is shown in purple. No attempt has been made to model the conformation of the 3′ acceptor strand of $tRNA^{Gln}$ onto the surface of Met-tRNA synthetase.

of the bottom part of the acceptor stem, the D stem, and the anticodon stem. The loop and β-strand that connect the two helices present a flat surface onto which is juxtaposed the extreme inside corner of the "L" of the tRNA. Proper orientation of the inside corner of $tRNA^{Gln}$ onto the protein structural surface formed by the loop, β-strand, and second α-helix of this motif then necessarily results in directing the acceptor stem and 3′-terminal CCA end toward the enzyme active site. The long second α-helix further orients the anticodon stem and loop of the tRNA adjacent to the β-barrel domains.

Superposition of the dinucleotide-fold domains of the enzymes results as well in a superposition of the first α-helix of the helix–turn–strand–helix motif, and therefore this helix has the same orientation in each enzyme (Table 1). However, inspection of Fig. 2 reveals that there is a divergence in the sizes of the intervening loop and strand structures and in the orientations of the long second helix (helix α-L of Gln-tRNA synthetase; helix α-H1 of Met-tRNA synthetase) relative to the superimposed dinucleotide folds. Despite this divergence, the striking overall similarity in the structure of the motif suggests that it might serve a common function in properly orienting the respective tRNA substrates. Superposition of the two dinucleotide-binding-fold motifs and subsequent adjustment of the position of the $tRNA^{Gln}$ molecule so that it interacts with the helix–turn–strand–helix motif of Met-tRNA synthetase in a manner analogous to its interaction with this motif in Gln-tRNA synthetase produces a preliminary model for the cognate Met-tRNA synthetase–$tRNA^{Met}$ interaction in which the anticodon of the tRNA is located directly adjacent to the C-terminal domain of Met-tRNA synthetase. This model suggests that the orientation of the second helix of the motif in each case determines the global positioning of the anticodon and D stems of the cognate tRNA.

We propose that in the Met-tRNA synthetase–$tRNA^{Met}$ complex the conserved α-helix–turn–β-strand–α-helix motif of Met-tRNA synthetase is similarly located at the inside corner of $tRNA^{Met}$ (Figs. 2 and 3). While no significant primary sequence similarity between Gln-tRNA synthetase and Met-tRNA synthetase can be discerned within this motif, in both enzymes the second helix possesses a strong net negative charge despite its location adjacent to the highly negatively charged phosphate backbone of the tRNA. In the Met-tRNA synthetase–$tRNA^{Met}$ model this helix lies along the entire length of the inside of the tRNA from the D stem to the anticodon stem, as is observed in the Gln-tRNA synthetase–$tRNA^{Gln}$ complex. Interestingly, in Gln-tRNA synthetase there are very few direct polar contacts made between the helix and the tRNA despite their relatively close proximity; however, a number of water-mediated interactions do occur. Residues 316–319 of Gln-tRNA synthetase form the sequence Thr-Lys-Gln-Asp and are located at the extreme inside corner of the "L" of the tRNA, making a number of side-chain hydrogen bonding interactions with the sugar-phosphate backbone. The region of Met-tRNA synthetase located at this position in the model (residues 356–360) forms the sequence Arg-Tyr-Tyr-Tyr-Thr and is thus similarly capable of polar interaction with the tRNA. This sequence is well-conserved in Met-tRNA synthetase enzymes from other organisms (25, 26).

In this model of the Met-tRNA synthetase–$tRNA^{Met}$ complex two protein "fingers" located adjacent to the major groove of the tRNA at the approximate location of the junction between the acceptor and T stems are seen. These fingers represent loops that are located in the insertion within the second half of the dinucleotide fold. Because the major groove of the A helix in RNA is very deep and narrow, these fingers probably cannot penetrate sufficiently far to allow direct recognition of base pairs in this region; all contact may thus be with the sugar-phosphate backbone. Recognition of functional groups of bases in double-stranded regions of $tRNA^{Gln}$ by Gln-tRNA synthetase is via protein contact in the minor groove of the acceptor stem, which is quite shallow allowing easy penetration of protein structural elements (13).

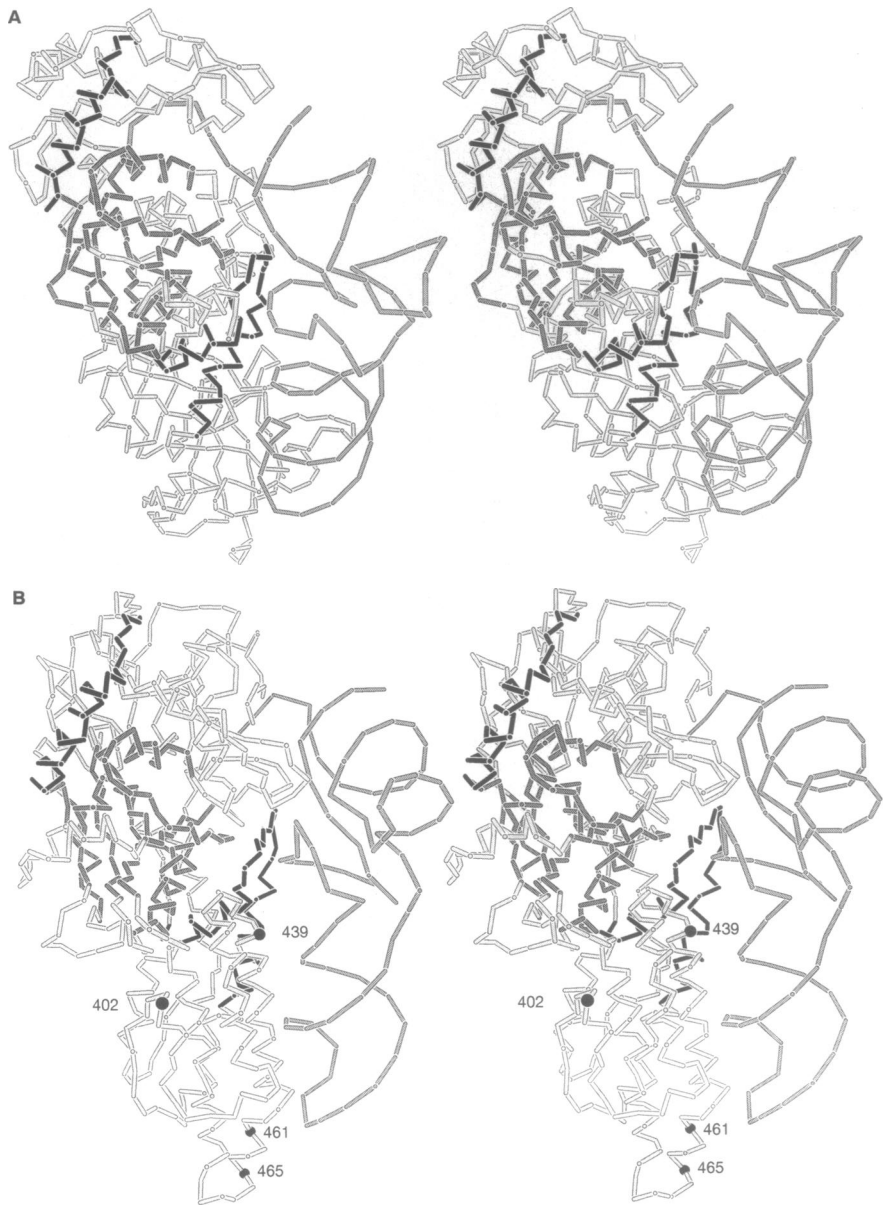

FIG. 3. (*A*) Stereoview of the Gln-tRNA synthetase-tRNA^{Gln} complex as seen in the cocrystal structure. The dinucleotide-fold domain is in dark gray and the two additional conserved motifs are shown in black. (*B*) Docking of tRNA^{Gln} on the surface of Met-tRNA synthetase. Proposed interaction of Met-tRNA synthetase along the entire inside of the L-shaped structure of tRNA^{Gln}, showing a similar overall topology of interaction as is seen for the Gln-tRNA synthetase–tRNA^{Gln} complex. The orientation of the acceptor stem relative to the dinucleotide fold is very similar to the orientation seen in the crystal structure of the Gln-tRNA synthetase–tRNA^{Gln} complex and is based on the structural homology between the respective dinucleotide-fold domains. The orientation of the anticodon stem is determined on the basis of the structural similarity between the two enzymes in the α-helix–turn–β-strand–α-helix motif (also see text), which in the Gln-tRNA synthetase–tRNA^{Gln} complex clearly serves to globally orient the tRNA onto the surface of the enzyme. This conserved motif at the inside corner of the tRNA is highlighted in black. Lysine and tryptophan residues of Met-tRNA synthetase that have been shown by biochemical means (19, 21, 24) to be in proximity to the anticodon and D loop are indicated by black dots. Two loops (closer loop residues 261–267, farther loop 235–237) of the Met-tRNA synthetase enzyme project into the major groove near the junction of the acceptor and T stems.

The lack of direct interaction of Met-tRNA synthetase in the minor groove of the acceptor stem of tRNA^{Met} predicted here is in accord with biochemical data that suggest that these base pairs can be altered with little effect on tRNA discrimination (27). No attempt has been made to model the conformation of the acceptor strand of the tRNA when bound to Met-tRNA synthetase. However, it appears likely that the single-stranded CCA end will form a hairpin-like structure in order to position the ribose moiety of the adenosine at position 76 in the active site. Bending of the 3′-terminal acceptor arm of tRNA^{fMet} towards the inside of the L-shaped tRNA has previously been suggested on the basis of singlet–singlet energy transfer experiments utilizing fluorescent-labeled forms of this tRNA (28).

In the proposed Met-tRNA synthetase–tRNA^{Met} model, the anticodon of the tRNA is positioned directly adjacent to an α-helix that is located in the C-terminal domain and contains amino acids previously implicated in recognition. Chemical cross-linking studies suggest that Lys-465 on this helix is within 14 Å of the anticodon of the tRNA (21), and site-directed mutagenesis data have further implied a role in binding for residue Trp-461 (19, 20). Lys-402 and Lys-439, located as well in the carboxyl-terminal helical domain, also have been implicated by chemical cross-linking (24). While in our model

Lys-439 is positioned within the 14-Å length of the cross-linker to the anticodon stem of the tRNA, Lys-402 is found on the opposite side of the enzyme. It is possible, however, that the cross-link to this residue occurred as a result of nonspecific interaction between different complexes that have the potential to form in solution. In this context we also note that mutation of this residue does not affect the ability of the enzyme to bind $tRNA^{Met}$ (L. Schulman, personal communication).

Several additional experiments are consistent with the overall orientation of tRNA on Met-tRNA synthetase that is proposed. Amino acids Lys-61 and Lys-335, identified by affinity-labeling studies utilizing 3′ end-modified forms of $tRNA^{Met}$ (17), are located near the proposed 3′ end of the tRNA model. Additionally, a number of peptide insertions into the domain that spans the two halves of the dinucleotide fold yielded modified enzymes that retain nearly full Met-tRNA synthetase activity (29). All of these insertions are located on surfaces of the enzyme located well away from the proposed area of tRNA interaction, consistent with the model. In contrast, insertion of amino acids into the loop (residues 149–160) that is located adjacent to the proposed binding site of the 3′ acceptor strand of the tRNA inactivates the enzyme (29).

We suggest that the similar mode of tRNA binding proposed for Gln-tRNA synthetase and Met-tRNA synthetase may also be observed in some other aminoacyl-tRNA synthetase RNA complexes. The occurrence of a structurally similar dinucleotide-fold domain among three (Gln-tRNA, Met-tRNA, and Tyr-tRNA synthetases) of the nine synthetases possessing both the His-Ile-Gly-His and Lys-Met-Ser-Lys-Ser motifs suggests the possibility that this structure is found among the other enzymes in the subclass as well. Eight of these enzymes (Gln-tRNA, Met-tRNA, Trp-tRNA, Glu-tRNA, Ile-tRNA, Val-tRNA, Leu-tRNA, and Arg-tRNA synthetases) bind one tRNA per enzyme subunit; the latter six may thus also possess the α-helix–turn–β-strand–α-helix motif and form tRNA complexes similar in overall topology to that observed in the Gln-tRNA synthetase–$tRNA^{Gln}$ crystal structure and proposed here for the Met-tRNA synthetase–$tRNA^{Met}$ interaction. The Tyr-tRNA synthetase enzyme, whose structure does not exhibit either of the two new motifs described here, is a dimeric synthetase that binds only a single tRNA molecule (30). The tRNA binding site spans the enzyme subunits (31), strongly suggesting that the overall orientation of binding will not resemble that described here. The discovery of sequence similarities among many of the synthetases that lack the His-Ile-Gly-His and Lys-Met-Ser-Lys-Ser motifs (32) and the novel structure of Ser-tRNA synthetase (33) indicate the existence of a second subclass of these enzymes that is organized along quite different structural principles than those described here.

The proposed interaction between Met-tRNA synthetase and $tRNA^{Met}$ is consistent with most of the available biochemical and genetic data and makes additional predictions that may be experimentally tested. Ultimately, crystal structures of this and other synthetase–tRNA complexes will be necessary to fully ascertain the general structural principles governing recognition of and discrimination between tRNAs by aminoacyl-tRNA synthetases.

We thank LaDonne Schulman for helpful discussions and critical reading of the manuscript. This work was supported in part by National Institutes of Health Grant GM-22778 to T.A.S.

1. Schimmel, P. (1987) *Annu. Rev. Biochem.* **56**, 125–158.
2. Yamao, F., Inokuchi, H., Cheung, A., Ozeki, H. & Sill, D. (1982) *J. Biol. Chem.* **257**, 11639–11643.
3. Breton, R., Sanfacon, H., Papayannopoulos, I., Biemann, K. & LaPointe, J. (1986) *J. Biol. Chem.* **261**, 10610–10617.
4. Winter, G., Koch, G. L. E., Hartley, B. S. & Barker, D. G. (1983) *Eur. J. Biochem.* **132**, 383–387.
5. Hall, C. V., van Cleemput, M., Muench, K. H. & Yanofsky, C. (1982) *J. Biol. Chem.* **257**, 6132–6136.
6. Dardel, F., Fayat, G. & Blanquet, S. (1984) *J. Bacteriol.* **160**, 1115–1122.
7. Webster, T., Tsai, H., Kula, M., Mackie, G. A. & Schimmel, P. (1984) *Science* **226**, 1315–1317.
8. Haertlein, M., Frank, R. & Madern, D. (1987) *Nucleic Acids Res.* **15**, 9081–9082.
9. Haertlein, M. & Madern, D. (1987) *Nucleic Acids Res.* **15**, 10199–10210.
10. Eriana, G., Dirheimer, G. & Gangloff, J. (1989) *Nucleic Acids Res.* **17**, 5725–5736.
11. Hountondji, C., Dessen, P. & Blanquet, S. (1986) *Biochimie* **68**, 1071–1078.
12. Heck, J. D. & Hatfield, G. W. (1988) *J. Biol. Chem.* **263**, 868–877.
13. Rould, M. A., Perona, J. J., Soll, D. & Steitz, T. A. (1989) *Science* **246**, 1135–1142.
14. Brunie, S., Zelwer, C. & Risler, J.-L. (1990) *J. Mol. Biol.* **216**, 411–424.
15. Brick, P., Bhat, T. N. & Blow, D. M. (1989) *J. Mol. Biol.* **208**, 83–98.
16. Labouze, E. & Bedouelle, H. (1989) *J. Mol. Biol.* **205**, 729–735.
17. Hountondji, C., Blanquet, S. & Lederer, F. (1985) *Biochemistry* **24**, 1175–1180.
18. Mechulam, Y., Dardel, F., Le Corre, D., Blanquet, S. & Fayat, G. (1991) *J. Mol. Biol.*, in press.
19. Ghosh, G., Pelka, H. & Schulman, L. H. (1990) *Biochemistry* **29**, 2220–2225.
20. Meinnel, T., Mechulam, Y., Le Corre, D., Panvert, M., Blanquet, S. & Fayat A. (1991) *Proc. Natl. Acad. Sci. USA* **88**, 291–295.
21. Leon, O. & Schulman, L. H. (1987) *Biochemistry* **26**, 5416–5422.
22. Schulman, L. H. & Pelka, H. (1988) *Science* **242**, 765–768.
23. Rossman, M. G. & Argos, P. (1976) *J. Mol. Biol.* **105**, 75–95.
24. Valenzuela, D. & Schulman, L. H. (1986) *Biochemistry* **25**, 4555–4561.
25. Walter, P., Gangloff, J., Bonnett, J., Boulanger, Y., Ebel, J. P. & Fasiolo, F. (1983) *Proc. Natl. Acad. Sci. USA* **80**, 2437–2441.
26. Tzagoloff, A., Vambutas, A. & Akai, A. (1989) *Eur. J. Biochem.* **179**, 365–371.
27. Schulman, L. H. (1990) *Prog. Nucleic Acids Res. Mol. Biol.* **41**, in press.
28. Ferguson, B. Q. & Yang, D. C. H. (1986) *Biochemistry* **25**, 6572–6578.
29. Starzyk, R. M., Burbaum, J. J. & Schimmel, P. (1989) *Biochemistry* **28**, 8479–8484.
30. Dessen, P., Zaccai, G. & Blanquet, S. (1982) *J. Mol. Biol.* **159**, 651–664.
31. Ward, H. J. W. & Fersht, A. R. (1988) *Biochemistry* **27**, 5525–5530.
32. Eriani, G., Delarue, M., Poch, O., Gangloff, J. & Moras, D. (1990) *Nature (London)* **347**, 203–206.
33. Cusack, S., Berthet-Colominas, C., Haertlein, M., Nassar, N. & Leberman, R. (1990) *Nature (London)* **347**, 249–255.